IEEE Access
Multidisciplinary | Rapid Review | Open Access Journal

Received December 6, 2020, accepted December 23, 2020, date of publication December 30, 2020,
date of current version January 12, 2021.

Digital Object Identifier 10.1109/ACCESS.2020.3048153

A Novel Method for Detecting Characteristic Parameters of Coating Layers by Ultrasonic Surface Wave Technique

WEIMING CAI[1], BO ZHANG[2], KAI ZHENG[2], YUPENG WU[2], AND YITAO ZHANG[1,3]
[1]School of Information Science and Engineering, NingboTech University, Ningbo 315100, China
[2]Institute of Metal Research, Chinese Academy of Sciences, Shenyang 110016, China
[3]College of Control Science and Engineering, Zhejiang University, Hangzhou 310058, China

Corresponding author: Bo Zhang (zb@imr.ac.cn)

This work was supported in part by the National Natural Science Foundation of China under Grant 51605468, Grant 31702393, and Grant 32073028; and in part by the Ningbo Public Welfare Key Project under Grant 2019C10098 and Grant 2019B10079.

ABSTRACT An improved reversion method for ultrasonic surface wave characterization of coating layers is presented and validated by experiment. The experiment is implemented with seven specimens of thin Cu layers coated on Al substrates. 2-D Fourier transforms of the experimentally obtained surface wave pulse propagation signals were conducted to obtain frequency-wave number relations. The combined equations of two unknowns were derived using the relation. The two unknowns are the thickness h and the Young's modulus E of the coating layer of the specimen. The h and E are obtained by solution of the combined equations. Comparing with that used for many years which are based on 1-D Fourier transform and non-linear regression, the new method is simpler, faster, and equally accurate and reliable. The standard error of 1.55μm is reached in the measurements of the Cu films thicknesses which vary in the range from 23.6μm to 224.8μm. The standard error of 2.97GPa is reached in measurements of Young's modulus of the Cu films and the exact value of Young's modulus of pure Cu is 110GPa.

INDEX TERMS 2-D Fourier transform, coating layers, ultrasonic variables measurement, nondestructive testing.

I. INTRODUCTION

The Modern surface coating technology is an effective way to improve the resistances of materials against fatigue, wear, corrosion, and oxidation at high temperature [1]–[4]. The improvement of the resistances extends significantly the life time of some important components which are used in industrial equipment, such as aircrafts, space flight vehicles, automobiles, oil recovery and petrochemical equipment, power station equipment [5]–[7]. Surface coating technology is of importance not only to traditional industries, but also to newly developed industries, for example semiconductor films for solar cells and transistors, ceramic films for superconductors, magnetic films for storage media, carbide and nitride coating layers for hardening and chemical resistivity of a surface, diamond-like films for superior mechanical and thermal properties, and so on [8]–[11].

The associate editor coordinating the review of this manuscript and approving it for publication was Xiaokang Yin.

Because of the important role of the coating layers and some occasional factors involved in the coating layers manufacturing, the non-destructive characterization (NDC) of the coating layers by detecting their characteristic parameters is necessary for quality control of products. In addition the characteristic parameters of coating layers are more or less related to their microstructure, homogeneity, defects and purity etc, so that non-destructive measurements of the characteristic parameters are useful for research of coating films.

For many years, ultrasonic surface wave technique for non-destructive characterization (NDC) of coating layers arouses interest of researchers due to the fact that the technique can be used to determine simultaneously up to three of the following four characteristic parameters of a coating layer: thickness, density, two elastic constants of homogeneous and isotropic coating layer. Especially it is possible to measure very thin films, such as 33nm thick Ag film on fused silicon, using ultrasonic surface wave method [11]. Recently the laser

generated ultrasonic surface wave (LSW) technique has been developed into a fast and reliable method for NDC of thine films on substrates [12]–[14].

A large percent of published papers dealing with the LSW NDC of films follow the general procedure. D Schneider evaluates diamond and diamond-like carbon films coated on (100) plane of silicon substrates [15]. How many parameters of a film can be determined simultaneously by LSW NDC is found dependent on the thickness of the film. The dependence shown by the experiment results is as follows. For the 0.08μm thick film only one parameter can be determined, for the 0.95μm and 1.2μm thick films two parameters of each film can be determined, for the 3.7μm thick film three parameters can be determined. In above mentioned determinations the bandwidth of the ultrasonic measurements is 200MHz. It is found that the Young's modulus of the diamond-like carbon film varies in a wide range. D Schneider measures the thickness and Young's modulus of nickel films coated on cemented carbide (W, Ti, Ta) C-Co substrates and TiC films coated on the same substrates by means of LSW technique [16]. D C Hurley develops a reversion algorithm for LSW NDC of layered anisotropic plates [17]. Five specimens of titanium nitride films coated on silicon single crystals are investigated. A Cheng calculates the dispersion curves of LSW in Ti film on Al substrate and in Al film on Ti substrate [18]. The dispersion curves plotted in the paper include not only the lowest mode in Ti/Al configuration and the lowest mode in Al/Ti configuration, but also the higher modes which are rarely seen in literatures [18]. B Knight investigates non-destructive evaluation of the adhesion between coating layer and substrate using LSW method [19]. Good adhesion is simulated by welding boundary condition and bad adhesion is simulated by boundary condition of very thin liquid layer coupling.

Usually the calculation of the dispersion curve using the known properties of the layer and the substrate is called forward calculation, whereas the calculation of the unknown properties of the layer using the measured dispersion curve and known properties of the substrate is called reverse calculation, or briefly reversion. The present paper is aimed at simplification of the inversion in LSW NDC of films. 2-D Fourier transform is used instead of phase velocity calculation to obtain the experimental *f-k* pattern immediately, which is equivalent to the *c-f* curve. Solution of combined equations is chosen instead of nonlinear regression to obtain the parameters of the layer coated on the substrate. Seven specimens of copper films coated on aluminum substrates are measured and calculated for validation of the improved reversion method. The thickness and Young's modulus of the film of each specimen measured by LSW method are compared with the thickness measured by metallographic microscope and with the Young's modulus measured ultrasonically with bulk copper specimen.

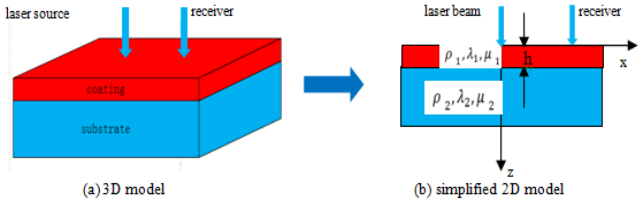

FIGURE 1. The model of the specimen of layer coated on substrate.

II. MATERIALS AND METHODS

A. THE MODEL OF THE LAYER COATED ON THE SUBSTRATE

The equations of potential functions for a two-dimensional elastic wave are:

$$\frac{\partial^2\varphi}{\partial t^2} = c_L^2\left(\frac{\partial^2\varphi}{\partial x^2} + \frac{\partial^2\varphi}{\partial z^2}\right) \tag{1}$$

$$\frac{\partial^2\psi}{\partial t^2} = c_S^2\left(\frac{\partial^2\psi}{\partial x^2} + \frac{\partial^2\psi}{\partial z^2}\right) \tag{2}$$

where φ denotes the scale potential, ψ denotes the vector potential, t denotes time, c_L denotes the velocity of longitudinal wave, c_S denotes the velocity of shear wave, x and z denote the coordinates of a point in the Cartesian coordinate system as shown in Fig.1.

The model of the layer coated on the substrate with the referred coordinate system is shown in Fig.1. The parameters of the layer and the substrate are given in Fig.1 by the characters: ρ denotes the density, λ and μ denote the Lama constants, foot note1 denotes the coating layer, foot note2 denotes the substrate. The thickness of the layer is denoted by h.

According to the model of the specimen shown in Fig.1 the boundary condition of the equations (1) and (2) is:

$$\sigma_{ZZ1} = 0, \quad \sigma_{ZX1} = 0, \ when\ z = 0 \tag{3}$$

$$\sigma_{ZZ1} = \sigma_{ZZ2}, \quad \sigma_{ZX1} = \sigma_{ZX2}, \ u_1 = u_2, \quad w_1 = w_2, \quad when\ z = h \tag{4}$$

where σ denotes stress, first foot note denotes the direction of the stress, second foot note denotes the normal of the plane on which the stress acts, u denotes the displacement in x direction, w denotes the displacement in z direction, foot note 1 denotes the coating layer, foot note 2 denotes the substrate. Solving equations (1) and (2) with boundary condition (3) and (4) leads to that determinate $|A|$ must be equal to zero. Equation $|A| = 0$ is called phase velocity dispersion equation,

$$|A| = \left|(A_{ij})\right| =, \quad i, j = 1, 2, 3 \ldots 6$$

$$A_{11} = ike^{-\eta_{L1}h}; \quad A_{12} = ike^{\eta_{L1}h}; \ A_{13} = \eta_{S1}e^{-\eta_{S1}h}$$

$$A_{14} = -\eta_{S1}e^{\eta_{S1}h}; \quad A_{15} = -ike^{-\eta_{L2}h}; \ A_{16} = -\eta_{S2}e^{-\eta_{S2}h}$$

$$A_{21} = -\eta_{L1}e^{-\eta_{L1}h}; \quad A_{22} = \eta_{L1}e^{\eta_{L1}h}; \ A_{23} = ike^{-\eta_{S1}h}$$

$$A_{24} = ike^{\eta_{S1}h}; \quad A_{25} = \eta_{L2}e^{-\eta_{L2}h}; \ A_{26} = -ike^{-\eta_{S2}h}$$

$$A_{31} = \lambda_1\left(\eta_{L1}^2 - k^2\right) + 2\mu_1\eta_{L1}^2$$

TABLE 1. Properties of the materials of the coating layers and the substrates measured with bulk specimens.

Specimens	Properties of 6061 Al and pure Cu			Coating method
	Density(kg/m^3)	Young's modules (GPa)	Passion ratio v	
6061 Al for 1#,2#,3#,4#	2734	83.7	0.31	electroplating
6061 Al for 5#,6#,7#	2738	71.3	0.349	sputter coating
Pure Cu for all specimens	8960	110	0.35	/

$$
\begin{aligned}
A_{32} &= \lambda_1\left(\eta_{L1}^2 - k^2\right) + 2\mu_1\eta_{L1}^2; \quad A_{33} = -2\mu_1 ik\eta_{S1} \\
A_{34} &= 2\mu_1 ik\eta_{S1}; \quad A_{35} = 0; A_{36} = 0 \\
A_{41} &= -2ik\eta_{L1}; \quad A_{42} = 2ik\eta_{L1}; \; A_{43} = -\left(k^2 + \eta_{S1}^2\right) \\
A_{44} &= -(k^2 + \eta_{S1}^2); \quad A_{45} = 0; A_{46} = 0 \\
A_{51} &= \left(\lambda_1\left(\eta_{L1}^2 - k^2\right) + 2\mu_1\eta_{L1}^2\right)e^{-\eta_{L1}h} \\
A_{52} &= \left(\lambda_1\left(\eta_{L1}^2 - k^2\right) + 2\mu_1\eta_{L1}^2\right)e^{\eta_{L1}h} \\
A_{53} &= -2\mu_1 ik\eta_{S1}e^{-\eta_{S1}h}; \quad A_{54} = 2\mu_1 ik\eta_{S1}e^{\eta_{S1}h} \\
A_{55} &= -\left(\lambda_2\left(\eta_{L1}^2 - k^2\right) + 2\mu_1\eta_{L1}^2\right)e^{-\eta_{L1}h} \\
A_{56} &= 2\mu_2 ik\eta_{S2}e^{-\eta_{S2}h} \\
A_{61} &= -2\mu_1 ik\eta_{L1}e^{-\eta_{L1}h}; \quad A_{62} = 2\mu_1 ik\eta_{L1}e^{\eta_{L1}h} \\
A_{63} &= -\mu_1\left(k^2 + \eta_{S1}^2\right)e^{-\eta_{S1}h} \\
A_{64} &= -\mu_1\left(k^2 + \eta_{S1}^2\right)e^{\eta_{S1}h}; \quad A_{65} = -2\mu_2 ik\eta_{L2}e^{-\eta_{L2}h} \\
A_{66} &= -\mu_1\left(k^2 + \eta_{S2}^2\right)e^{-\eta_{S2}h} \\
\eta_{L1} &= \sqrt{k^2(1 - \frac{c^2}{c_{L1}^2})}, \quad \eta_{S1} = \sqrt{k^2(1 - \frac{c^2}{c_{S1}^2})} \\
\eta_{L2} &= \sqrt{k^2(1 - \frac{c^2}{c_{L2}^2})}, \quad \eta_{S2} = \sqrt{k^2(1 - \frac{c^2}{c_{S2}^2})}
\end{aligned} \tag{5}
$$

where k denotes the wave number of the surface wave, c denotes the phase velocity of the surface wave.

B. CALCULATION OF DISPERSION CURVES

In order to know all aspects of the dispersion feature of the concerned coating layer and substrate combinations and to validate the dispersion Eq.(5) and calculation algorithms to be used in LSW NDC of the coating layers, the theoretical calculation and plot of the dispersion curves are necessary. Therefore the dispersion curves of the surface waves in Cu layers coated on Al substrates are calculated and plotted. The properties of the materials of the coating layers and the substrates, pure copper and 6061 aluminum alloy, are measured with bulk specimens. The measured values of the materials properties are listed in Table 1 and will be used in calculations of the dispersion curves.

Substituting the material properties values of the layer and the substrate listed in Table 1, the assumed layer thicknesses, and a series of assumed frequency fi(i = 1, 2, 3 . . . . .) into the dispersion equation that is Eq.(5) in the Appendix, the dispersion equations of surface waves propagating in Cu layers coated on Al substrates are obtained. The dispersion curves obtained by solution of above mentioned dispersion equations are shown in Fig.2. From the curves it is seen clearly that the thicker the coating layer, the steeper the curve descends with the increase of frequency. At the lowest frequency the phase velocity of the surface wave is equal to that of the Raleigh wave on Al surface and at the highest frequency the phase velocity is equal to that of the Raleigh wave on Cu surface.

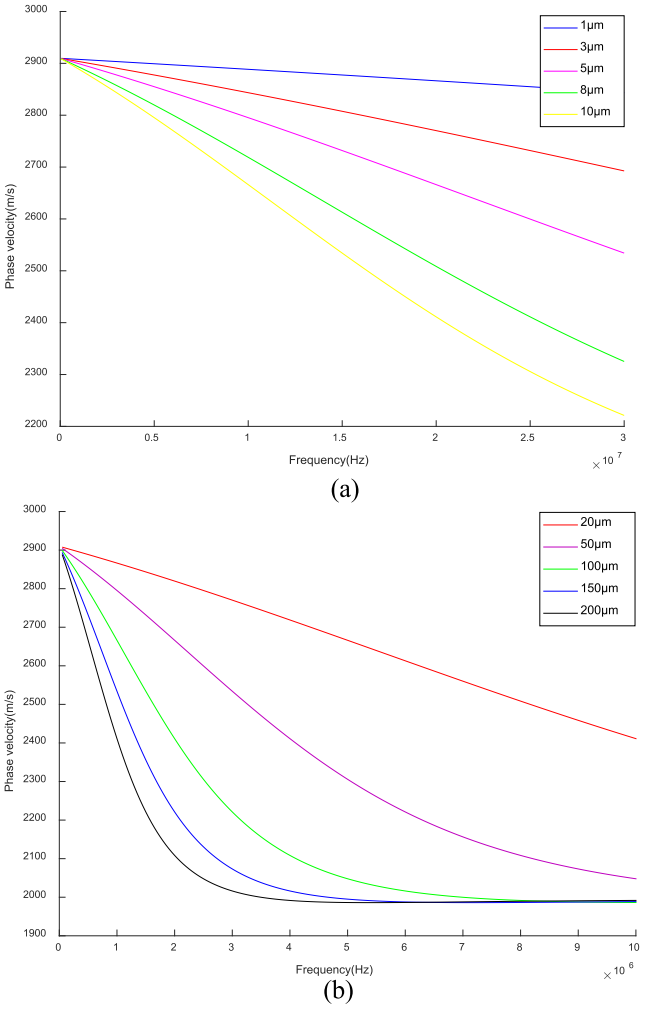

FIGURE 2. Dispersion curves of ultrasonic surface waves in Cu layers coated on Al substrates. (a) the thicknesses of the layers range from 1μm to 10μm (b) the thicknesses of the layers range from 20μm to 200μm.

TABLE 2. Properties of the materials of the coating layers and the substrates measured with bulk specimens.

Specimen number	Thickness measured by microscope h(μm)	Measured by LSW method		Used in reversion calculation			
		Thickness h(μm)	Young's modules E_1 (GPa)	frequency and wave number pairs			
				f_1(MHz)	k_1(1/m)	f_2(MHz)	k_2(1/m)
1#	23.6	25.2	111.7	3.22	6820	4.19	9083
2#	30.8	29.65	107.7	1.27	2588	3.12	6691
3#	40.1	39.8	108.8	1.09	2232	2.81	6161
4#	54.8	57.35	110.1	1.35	2851	2.02	4426
5#	75.4	76.25	104	1.24	2913	1.92	4752
6#	80	81.3	114	1.12	2611	1.7	4150
7#	224.8	225.5	110.4	1.18	3249	1.38	3923

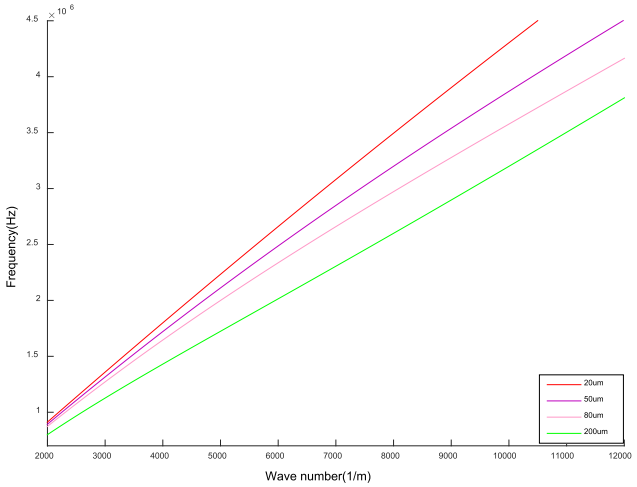

FIGURE 3. Dispersion curves of surface waves in Cu layers coated on Al substrates plotted in *f-k* coordinate system.

In order to facilitate the comparison of the theoretical dispersion curves with the dispersion patterns obtained by 2-D Fourier transform of the received LSW propagation signals, the theoretical curves plotted in c-f coordinate system are transformed into the equivalent curves plotted in f-k coordinate system, where k denotes wave number. In other words, the c-f curves are transformed into the equivalent f-k curves. The f-k curves are shown in Fig.3.

C. ACQUIREMENT OF SIGNALS OF SURFACE WAVE PULSES

The sensors in total seven specimens are prepared, four of them, 1#, 2#, 3#, 4# are prepared by electroplating and three of them, 5#, 6#, 7# are prepared by sputter coating. The substrates of the specimens have the same shape of rectangular solid and the same size of 100 × 50 × 10mm. The coating layers are made of pure copper and the substrates are made of 6061 aluminum alloy. The coating layer thicknesses of the specimens are in the range from 23.6μm to 224.8μm and the details of the specimens are listed in Table 2.

The experimental system used in the study of this paper consists of a pulsed laser whose pulse duration is less than

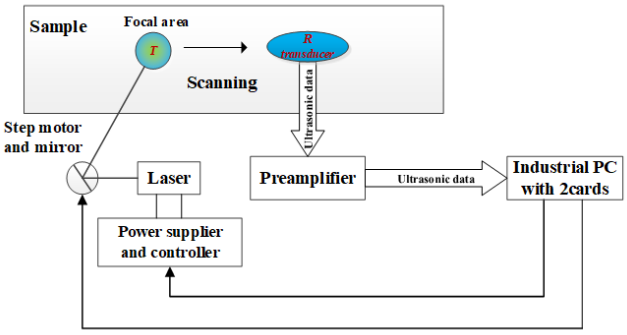

FIGURE 4. Laser ultrasonic measuring system.

10ns and energy per pulse is 10mJ, an ultrasonic receiving unite including a probe and a preamplifier, an industrial PC computer with two cards assembled into it, as shown in the Fig.3. The two cards are an A/D card and a reflecting mirror direction angle control card. The laser beam is focused on the specimen surface by a point-focal lens and the focal area on the specimen surface is of a round shape of 1.2mm diameter. The focal area is heated by the laser pulse and its temperature rises up suddenly, so that ultrasonic wave pulses, among which the surface wave pulse is the dominating component, are generated by thermal elastic mechanism. The ultrasonic probe is a popular angle beam probe consisted of a Perspex wedge and a piezoelectric disc. The beam angle of the refracted shear wave in steel generated by the probe is 70°. The central frequency of the probe is 4MHz. The surface wave pulse propagating in the coating layer of the specimen is received by the ultrasonic probe, amplified by the preamplifier, and transferred to the A/D card. The surface wave pulse is digitalized by the A/D card and stored in the IPC computer as time domain signal of the surface wave. The sampling frequency of the A/D is set at 66.66MHz. After a signal is stored, the laser beam is moved to the next focal area and above mentioned signal acquiring and storing is repeated ones again. The laser beam is moved to a series of focal areas one by one, meanwhile the laser generated surface wave pulses are received, processed and stored. In this way signal of surface wave propagation is obtained and the signal can be

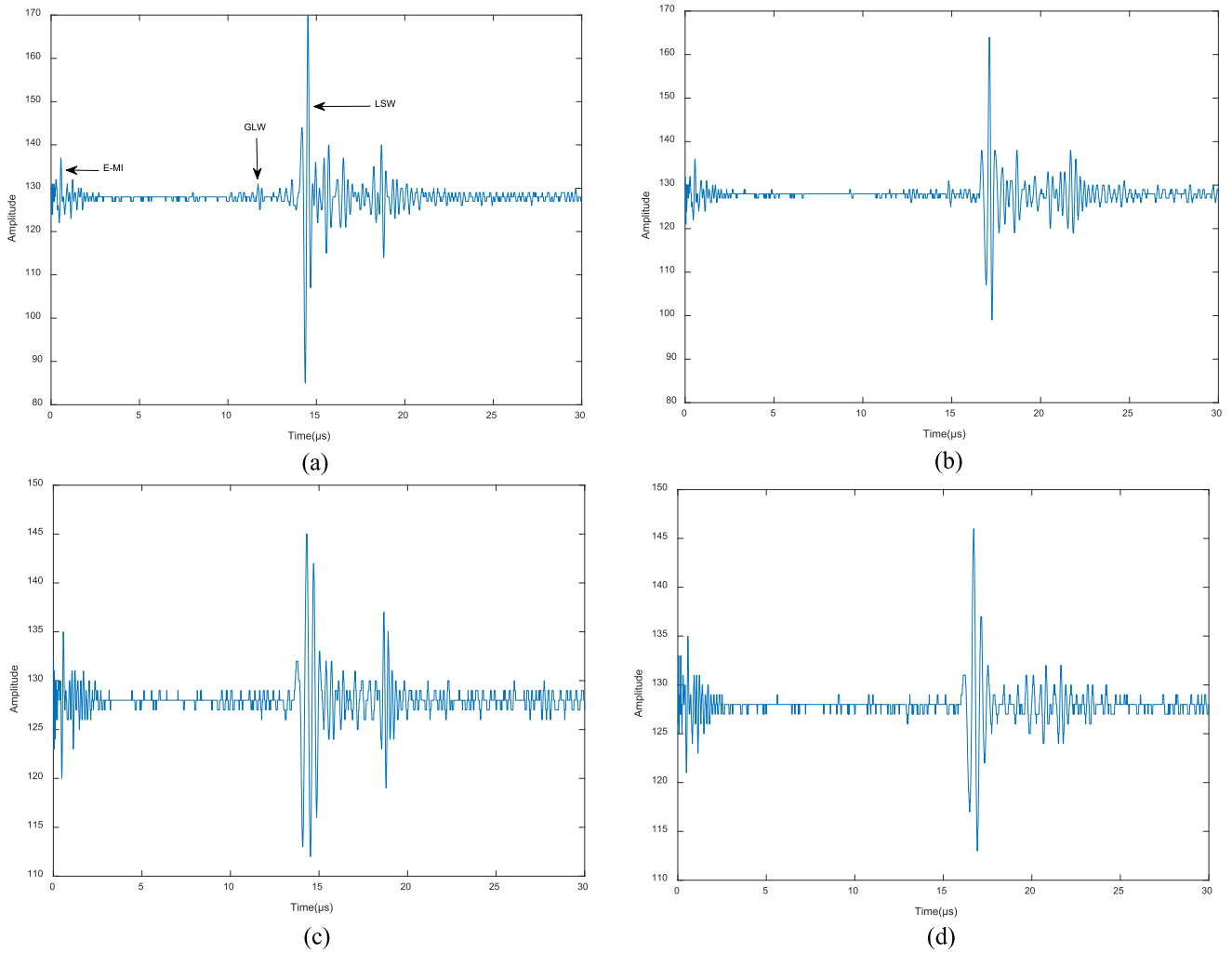

FIGURE 5. A-scan signals of LSWs propagating in coating layers of different specimens. The signals are received at different distances from the source. (a) Specimen 1#, at 40mm distance from the source (b) Specimen 1#, at 50mm distance from the source (c) Specimen 2 #, at 40mm distance from the source (d) Specimen2 #, at 50mm distance from the source.

denoted by:

$$Y = Y(x, t) \tag{6}$$

where Y denotes the signal amplitude, t denotes the time($t = 0$ means a laser light pulse is emitted), x is the distance from the probe to each of the focal areas. The focal areas are located in a line which coincides with the surface wave propagation path. The distance between two neighboring focal areas is 0.31mm. The movement of laser beam from one focal area to the next area is performed by the rotation of the reflecting mirror as shown in Fig.4. The rotation of the mirror is driven by a step motor controlled by the mirror angle control card. All of the mirror angle control, the data acquiring control, and the laser emission control are digital and programmable. The $Y = Y(x, t)$ data stored in the IPC computer are transferred to another computer for further procession. Some of the received A-scan signals of LSWs are shown in Fig.5. Besides the surface waves, the grazing longitudinal waves (GLW) and the electromagnetic interference from the power supplier of the laser (E-MI) are shown also in Fig.5.

D. CALCULATION OF THE THICKNESSES AND YOUNG'S MODULUS USING THE IMPROVED REVERSION METHOD

At first, seven small pieces are cut out from the seven specimens and the small pieces are prepared for metallographic measurements of the layer thicknesses. The layer thicknesses of the small pieces measured by metallographic microscope are listed in the second column of Table 2. Two metallographic pictures presented in Fig.6. show the layers appearances and thicknesses of the small pieces cut out from the specimen 5# and 7# respectively. After the metallographic observations and measurements, the coating layer thicknesses and Yung's modulus of the seven specimens are measured by LSW method. The procedure of LSW measurements on the specimens are as follows.

The signals of LSWs propagating in the seven specimens are acquired using the system shown in Fig.4. The

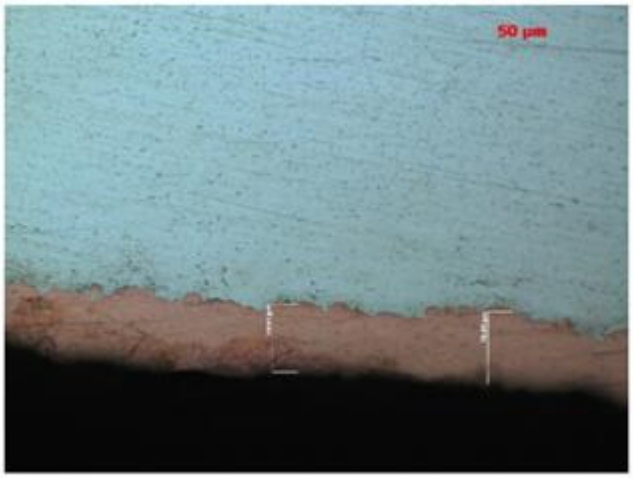

(a)specimen5#

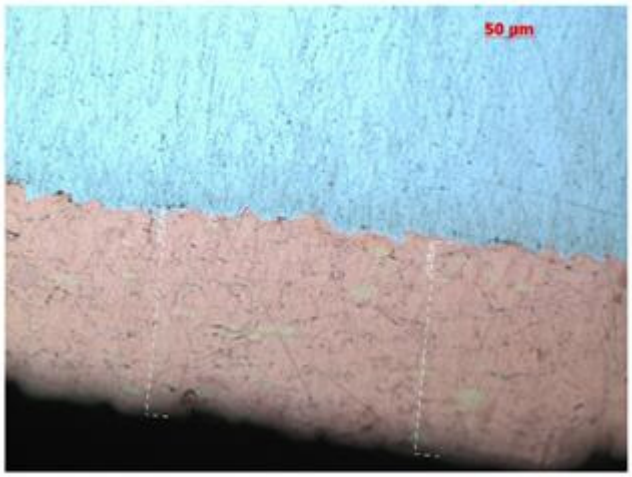

(b)specimen7#

FIGURE 6. Metallographic pictures showing the coating layers of specimens 5# and 7#, (a) specimen5# (b) specimen7#.

acquirement process is explained in detail in the paragraph three. 2-D Fourier transforms of the time domain wave propagation signals obtained by LSW measurements are made and the results are shown in Fig.6. Referring to equation (1), the transform can be expressed by the equation.

$$FY(x,t) = \int_{-\infty}^{\infty}\int_{-\infty}^{\infty} Y(x,t)e^{j\omega t}e^{-kx}dtdx \tag{7}$$

In Fig.7 the contours display the results of 2-D Fourier transform of the experimental $Y(x,t)$ signals. Four A-scan signals received at $x = 40$mm and $x = 50$mm are shown in Fig.4. The contours show three strip regions: the left region nearby the vertical axis displays the electro-magnetic interference from the power supplier of the laser (E-MI); the middle region displays the grazing longitudinal wave (GLW); the right region displays the dispersion pattern of the surface wave (LSW) in the Cu coating layer of the specimen. Observing the right strip region, two points which are on the center line of the region are chosen artificially for use in reversion calculation of the thickness and Young's modulus of the coating layer. The coordinates of the two chosen points are expressed by f_1-k_1 and f_2-k_2, and the values of them for each specimen are listed in right four columns of Table 2. For example, the two points chosen from the dispersion pattern obtained by 2-D Fourier transform of the surface wave propagating in specimen 7# have coordinate values $f_1 = 1.18$(MHz), $k_1 = 3249$(1/m), $f_2 = 1.38$(MHz), $k_2 = 3923$(1/m). Substituting the values of f_1-k_1 and f_2-k_2 pairs, i.e. 1.18(MHz)-3249(1/m) and 1.38(MHz)-3923(1/m), into Eq.(1) presented in the Appendix, the combined equations of two unknowns, which are the thickness h and Young's modulus E of the Cu layer, are obtained. The brief form of the combined equations can be written as:

$$|h, E, f_1, k_1| = 0 \tag{8}$$
$$|h, E, f_2, k_2| = 0 \tag{9}$$

The thickness h and Young's modulus E of the Cu layer obtained by solving the combined equations numerically are listed in the third and fourth column of Table 2. Substituting back the h and E obtained by solution of the combined equations into Eq.(5) and also substituting a series of assumed frequencies $f_i (i = 1, 2, 3, \ldots\ldots)$ into the equation, then the equations of the unknowns $k(f_i)$, which are the wave numbers of the surface wave propagating in the Cu coating layer, are established. Solving the established equations the $k(f_i)$-f_i relation is obtained. The $k(f_i)$-f_i relation is plotted as a dispersion curve together with the corresponding dispersion patterns obtained by 2-D Fourier transform of the experimental wave propagation signal. The above mentioned plots are shown in Fig.7. Fig.7 demonstrates that the dispersion curves are in good agreement with the dispersion patterns obtained by 2-D Fourier transform of the experimental LSW propagation signals.

III. DISCUSSION

The thicknesses of the Cu layers coated on the Al substrates measured by LSW and by microscope are listed in Table 2 and plotted in Fig.8. From the comparison of the thicknesses measured by LSW with those measured by microscope and observation of Fig.8, it could be seen that the agreement between the two groups of thicknesses obtained by two different methods is very good. Regarding the thicknesses measured by microscope as the true thicknesses, the root mean square (RMS) error of the film thicknesses measured by LSW is 1.55μm. In the film thickness range from 20μm to 220μm the error of film thickness measured by LSW is independent of the thickness of the measured film. Regarding the Young's modulus measured with bulk Cu specimen as the true one, the RMS error of the Young's modulus measured by LSW is 2.97GPa. No systematic difference between the Young's modulus of the Cu coating layers and that of the bulk Cu is found, if the measurement errors are taken into account. Comparison of the film thickness and Young's modulus measurement errors of this study with the errors of the similar measurements reported by journal papers, demonstrates that

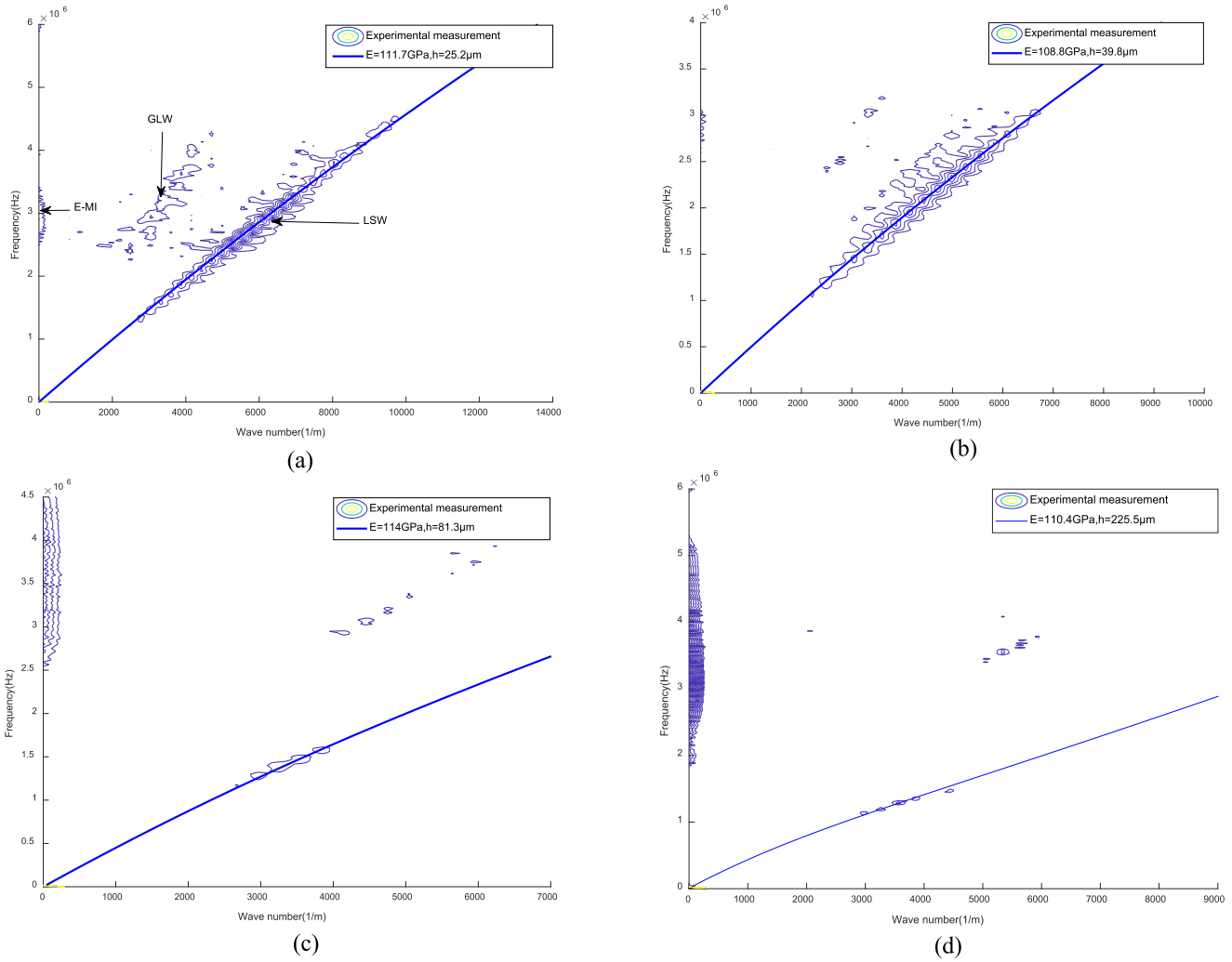

FIGURE 7. **Dispersion patterns obtained by 2-D Fourier transform of surface waves propagating in the coating layers of the four specimens and corresponding theoretically calculated dispersion curves, (a) specimen 1# (b) specimen 3# (c) specimen 6# (d) specimen 7#.**

the accuracy of measurement method developed by this study is the same as that of the previous method reported in journal papers [16]. Considering that the improved reversion method is used for reverse calculation of this study and the method is different from the previous reversion method reported by other journal papers, it could be concluded that the new reversion method reaches nearly the same accuracy and reliability as those the previous reversion method reaches.

The advantages of the new reversion method are simplification of the algorithm and reduction of the computation time. The new method consists of 2-D Fourier transform of the LSW propagation signal and solution of combined equations for reversion of the thickness and Young's modulus, whereas the previous method consists of the 1-D Fourier transform and nonlinear regression for reversion. The frequency and wave number relation, *f-k* relation, can be obtained immediately by 2-D Fourier transform of the experimental LSW propagation signal and the thickness and Young's modulus can be obtained by solution of combined equations. The above transform and solution can be done by two simple MATLAB programs. However to obtain the experimental *c-f* curve by 1-D Fourier transform and to finish the reverse calculation by nonlinear regression, much more work should be completed, including elimination of the phase uncertainty in determination of the phase difference between the two signals received at two source–receiver distances, and minimization of the differences between theoretical and experimental phase velocity dispersion curves for the nonlinear regression [16]. To obtain the *c-f* curve and to finish the nonlinear regression, besides the 1-D Fourier transform program two specially developed computation programs are necessary. Briefly the new method simplifies effectively the algorithms. In general, comparing with the previous inversion method, the improved inversion method is simpler, faster, equally accurate and reliable.

The disadvantage of the new reversion method is that two pairs of f and k should be chosen artificially according to the *f-k* contour graph obtained by 2-D Fourier transform, refer to Fig.6. Note that for getting three parameters of a

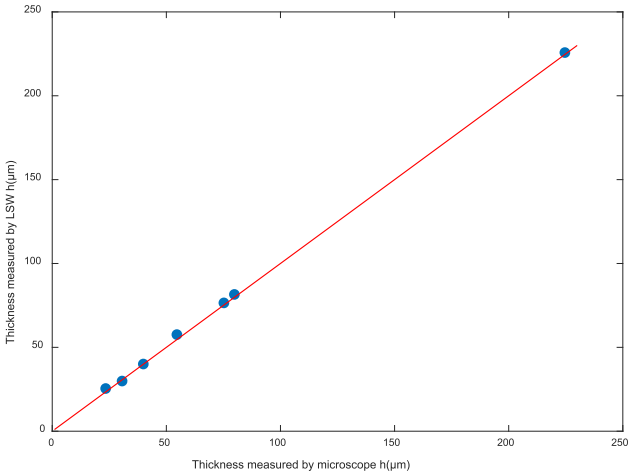

FIGURE 8. Comparison between the film thicknesses measured by LSW and those measured by microscope.

film three pairs of f and k are needed. Although the f-k relation obtained by 2-D Fourier transform and displayed by contour graph does not appear as a mathematical curve but a string of small areas where the surface wave is strongest, refer to Fig.7, the small areas are tiny enough for drawing a precise curve through the centers of the small areas. Therefore the artificial factor does not carry any significant error into the parameters measurements. Above opinion is supported by the fact that the accuracies of the thickness and Young's modulus measurements by the improved inversion method are equal to those by the previous reversion method.

IV. CONCLUSION

This paper proposed a novel method for detecting characteristic parameters of coating layers by ultrasonic surface wave technique. The surface wave pulse propagation signals were obtained by the experiment which was implemented with seven specimens of thin Cu layers coated on Al substrates. The combined equations of two unknowns are derived using the relation by 2-D Fourier transforms. Compared to the traditional method, such as 1-D Fourier transform and non-linear regression, the new method is simpler, faster, and equally accurate and reliable. The above transform and solution can be done by two simple MATLAB programs, but the traditional method needs more work, including two specially developed computation programs. The disadvantage of the new reversion method is that two pairs of f and k should be chosen artificially according to the f-k contour graph obtained by 2-D Fourier transform, which could bring some additional errors. That is a problem we have to resolve in the future.

ACKNOWLEDGMENT

The authors would like to thank NDT project team of IMR (Institute of Metal Research, Chinese Academy of Sciences) for profitable recommendations for improving method. They also thank the graduate student of IMR, Miss Lijun Zhou, for her effort and success in making the good coating layers of the specimens which are used in the study of the present paper.

REFERENCES

[1] S. Zhan, M. H. Azarian, and M. G. Pecht, "Surface insulation resistance of conformally coated printed circuit boards processed with no-clean flux," *IEEE Trans. Electron. Packag. Manuf.*, vol. 29, no. 3, pp. 217–223, Jul. 2006, doi: 10.1109/TEPM.2006.882496.

[2] I. Shahzadi, M. Bashir, S. Bashir, and M. H. Inayat, "Thermally assisted coating of PVA for hydrophilic surface modification of PMMA microchannel for oil in water emulsion," in *Proc. 15th Int. Bhurban Conf. Appl. Sci. Technol. (IBCAST)*, Islamabad, Pakistan, Jan. 2018, pp. 51–54, doi: 10.1109/IBCAST.2018.8312204.

[3] Y. Liu, Z. Lin, K. Moon, and C. P. Wong, "Superhydrophobic nanocomposite coating for reliability improvement of microelectronics," *IEEE Trans. Compon., Packag., Manuf. Technol.*, vol. 3, no. 7, pp. 1079–1083, Jul. 2013, doi: 10.1109/TCPMT.2013.2245724.

[4] K. Chaudhary, G. Singh, J. Ramkumar, S. Anantha Ramakrishna, K. V. Srivastava, and P. C. Ramamurthy, "Optically transparent protective coating for ITO-coated PET-based microwave metamaterial absorbers," *IEEE Trans. Compon., Packag., Manuf. Technol.*, vol. 10, no. 3, pp. 378–388, Mar. 2020, doi: 10.1109/TCPMT.2020.2972911.

[5] B. Behrens and M. Müller, "Technologies for thermal protection systems applied on re-usable launcher," *Acta Astronautica*, vol. 55, nos. 3–9, pp. 529–536, Aug. 2004.

[6] Y.-Y. Chang and C.-J. Wu, "Mechanical properties and impact resistance of multilayered TiAlN/ZrN coatings," *Surf. Coatings Technol.*, vol. 231, pp. 62–66, Sep. 2013.

[7] F. Cheng and S. Jiang, "Cavitation erosion resistance of diamond-like carbon coating on stainless steel," *Appl. Surf. Sci.*, vol. 292, pp. 16–26, Feb. 2014.

[8] M. H. Kang, D. K. Heo, D. H. Kim, M. Lee, K. Ryu, Y. H. Kim, and C. Yun, "Fabrication of spray-coated semitransparent organic solar cells," *IEEE J. Electron Devices Soc.*, vol. 7, pp. 1129–1132, 2019, doi: 10.1109/JEDS.2019.2949685.

[9] J. Zhao, A. Wang, and M. A. Green, "Double layer antireflection coating for high-efficiency passivated emitter silicon solar cells," *IEEE Trans. Electron Devices*, vol. 41, no. 9, pp. 1592–1594, Sep. 1994, doi: 10.1109/16.310110.

[10] L. Ding, J. Zhao, Y. Huang, W. Tang, S. Chen, and X. Guo, "Flexible-blade coating of small molecule organic semiconductor for low voltage organic field effect transistor," *IEEE Electron Device Lett.*, vol. 38, no. 3, pp. 338–340, Mar. 2017, doi: 10.1109/LED.2017.2657651.

[11] A. Neubrand and P. Hess, "Laser generation and detection of surface acoustic waves: Elastic properties of surface layers," *J. Appl. Phys.*, vol. 71, no. 1, pp. 227–238, Jan. 1992.

[12] C. Grunsteidl, J. Roither, I. A. Veres, B. Reitinger, T. Berer, H. Grun, P. Burgholzer, H. Kostenbauer, J. Winkler, H. Traxler, I. A. Veres, T. Berer, and P. Burgholzer, "Characterization of thin layers using a frequency domain laser-ultrasonic system," in *Proc. IEEE Int. Ultrason. Symp.*, Dresden, Germany, Oct. 2012, pp. 1734–1737, doi: 10.1109/ULTSYM.2012.0435.

[13] X. Xiao, B. Gao, and G. Y. Tian, "Investigation of ultrasonic NDT for small diameter and thin-wall tube," in *Proc. IEEE Int. Instrum. Meas. Technol. Conf. (I2MTC)*, Auckland, New Zealand, May 2019, pp. 1–5, doi: 10.1109/I2MTC.2019.8826968.

[14] B. Rocks, F. Gaudenzi, D. Irving, and D. A. Hughes, "Fully-flexible thin-film ultrasonic array for use in industrial NDE applications," in *Proc. IEEE Int. Ultrason. Symp. (IUS)*, Glasgow, U.K., Oct. 2019, pp. 2493–2495, doi: 10.1109/ULTSYM.2019.8925867.

[15] D. Schneider, T. Schwarz, H.-J. Scheibe, and M. Panzner, "Non-destructive evaluation of diamond and diamond-like carbon films by laser induced surface acoustic waves," *Thin Solid Films*, vol. 295, nos. 1–2, pp. 107–116, Feb. 1997.

[16] D. Schneider, T. Schwarz, and B. Schultrich, "Determination of elastic modulus and thickness of surface layers by ultrasonic surface waves," *Thin Solid Films*, vol. 219, nos. 1–2, pp. 92–102, Oct. 1992.

[17] D. C. Hurley, V. K. Tewary, and A. J. Richards, "Thin-film elastic-property measurements with laser-ultrasonic SAW spectrometry," *Thin Solid Films*, vols. 398–399, pp. 326–330, Nov. 2001.

[18] A. Cheng, T. W. Murray, and J. D. Achenbach, "Simulation of laser-generated ultrasonic waves in layered plates," *J. Acoust. Soc. Amer.*, vol. 110, no. 2, pp. 848–855, Aug. 2001.

[19] B. Knight, "Coating evaluation using analytical and experimental dispersion curves," in *Proc. AIP Conf.*, 2000, vol. 509, no. 1, pp. 263–270.

WEIMING CAI received the Ph.D. degree from Zhejiang University. From 2012 to 2013, he studied at Oklahoma State University. He is currently an Associate Professor of electric and electrical engineering. He also works as the Head of the Institute of Information and Electronic Technology, NingboTech University.

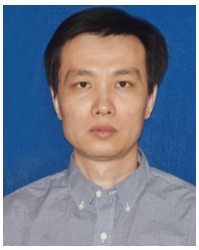

BO ZHANG received the Ph.D. degree in mechatronic engineering from the Shenyang Institute of Automation, Chinese Academy of Sciences. His main research interest includes industrial intelligent inspection theory and method.

KAI ZHENG received the bachelor's degree in metallic materials engineering from the Hefei University of Technology, in 2018. He is currently pursuing the master's degree in material processing engineering with the School of Materials Science and Engineering, University of Science and Technology. He is also a joint-raining graduate student with the Institute of Metal Research, Chinese Academy of Sciences, Shenyang. His main research interests include non-destructive testing and evaluation of materials.

YUPENG WU received the bachelor's degree in material chemistry from the Taiyuan University of Technology, in 2017. From 2017 to 2020, he has studied in material engineering with the School of Materials Science and Engineering, University of Science and Technology. His main research interests include non-destructive testing and evaluation of materials.

YITAO ZHANG received the bachelor's degree in automation from the Hefei University of Technology, in 2019. He is currently pursuing the master's degree in control engineering with the College of Control Science and Engineering, Zhejiang University. His main research interests include intelligent detection technology.